Passive Inerter-Based Network Self-Induced Oscillations Damping for Spar-Buoy Floating Offshore Wind Turbines

1st Sandra Piernikowska
School of Science & Technology
City, University of London
London, UK
sandra.piernikowska@city.ac.uk

2nd María Tomás-Rodríguez
School of Science & Technology
City, University of London
London, UK
maria.tomas-rodriguez.1@city.ac.uk

***Abstract*—This contribution analyses the influence of a passive inerter-based network on the stability of the 5MW NREL FOWT with a spar-buoy foundation when the system is subjected to the specific problem of self-induced oscillations. In this work, the idea of incorporating an inerter-based network with a classic tuned mass damper (TMD) in the nacelle is explored. The main objective is to show the effectiveness of the introduced network and demonstrate its benefit in the reduction of the oscillation amplitude when self-induced instabilities occur in comparison to the model equipped with TMD-only. It was demonstrated that the inerter-based network reduces the oscillation amplitude by over 90% and assures system stability when the loss of platform damping occurs.**

***Index Terms*—FOWT, TMD, inerter, self-induced oscillations**

I. INTRODUCTION

Wind energy belongs to the group of renewables together with solar energy or hydrogen. In the current energy market, the main objectives are to ensure a sufficient amount of energy is widely available to the customer at a reasonable price but also to face climate challenges related to global warming and the evident exhaustion of natural resources.

Offshore wind technology, in particular floating offshore wind turbines (FOWT), offers promising solutions to the global energy market challenges. FOWT are energy-generating marine structures which carry all the benefits of the onshore and fixed offshore technology such as environmental friendliness, cost-effectiveness and reliability. Due to their location in deep and open water, the FOWTs can be built larger in size and produce up to 30% more electricity than OWTs. FOWTs can entirely benefit from offshore natural resources in the form of much stronger and more constant winds as over 80% of these resources are available in the coastal waters where fixed foundations are no longer feasible [1], [2].

One of the main control objectives of wind technology is the maximization of power production. With FOWTs being much larger in size and exposed to harsher environmental factors, with no fixed foundation, another important stability objective arises as a consequence of the new challenges faced by a structure. One of the instabilities that the FOWT can experience are self-induced oscillations. Self-induced oscillations are a naturally occurring phenomenon, and in the case of FOWTs, they can appear due to the loss of floating platform damping.

Structural control, among others, is one of the methods of controlling the vibrational response in wind turbines. It was originally adapted from civil engineering applications [3]–[5]. One of the most widely used structural control devices is a tuned damper (TD) with a tuned mass damper (TMD) being favoured in wind turbine applications. TMD is a mechanical device consisting of a mass element, spring and damper. The device can be designed to be passive, semi-active or active with the passive TMDs popularized due to its simplicity and lack of energy input necessary [6], [7].

[8] studies a modelling and parameter tuning of a passive nacelle-based TMD for a 5MW NREL FOWT with an OC3-Hywind spar-buoy foundation. The authors analyse the relationship between spring and damper coefficients and the operating regions in power production. It was concluded that small spring and damping coefficients resulted in desirable load reduction in the above-rated wind region, however, the same values in the below-rated wind region caused the performance drop. It was also demonstrated that the selection of large spring and damping coefficients produced moderate load reduction in all working conditions.

Another structural control device which can also be implemented in FOWT is a tuned liquid damper (TLD). [9] numerically investigated the effectiveness of an implementation of a multilayer TLD in a spar-type FOWT to control a pitch motion.

An inerter is a mechanical device developed in the early 2000s by Professor Smith. An inerter works by exerting an equal and opposite force at its terminals which is proportional to the relative acceleration between them. The device has the constant of proportionality referred to as inertance, expressed in units of kilogram [10], [11]. The inerter can be used as a standalone element or can be connected in various topologies

*This research is funded by a 3-year Doctoral Studentship from the City, University of London, London. This work has been partially supported by the Spanish Ministry of Science and Innovation under project MCI/AEI/FEDER number PID2021-123543OBC21.

such as in combination with classic TMD either in series or parallel, referred to as TMDI or by the design of inerter-based networks [12].

[13] analyses the effects of a tuned mass damper inerter (TMDI) on vibrational suppression of FOWT tower with a spar-buoy foundation. The authors performed a parametric study on the mass ratio (ratio of TMD damper mass to the mass of the primary structure) and inertia ratio (ratio of the inertance to the mass of the primary structure). It was demonstrated that the performance of a TMDI improves for a fixed mass ratio with an increasing inerter ratio (up to 0.4) and that TMDI reduces stroke of tuned mass and tower top displacement.

[14] studies the spar-buoy FOWT structural reliability looking from the perspective of vibrational control when the system's tower is equipped with TMDI. A nonlinear 22DOFs system under the investigation is subjected to the misaligned wave-wind loadings. It was found that the introduction of the TMDI mitigates the vibrations of the tower which results in improvements to the system's reliability of over 90% in the rough met-ocean conditions. It was concluded that due to structural control of the TMDI in the tower, the consequent maintenance cost and power fluctuations can be also reduced.

[15] looks at the application of a tuned mass damper fluid-inerter (TMDFI) for vibration control in the FOWT tower with a spar-buoy foundation where the inerter is incorporated in parallel with a TMD in the nacelle. It was demonstrated that a fluid-inerter can perform as the ideal mechanical inerter and it is benficial in wind-wave load mitigation.

[16] investigates an inerter-enhanced vibration absorber i.e., a rotational inertia double-tuned mass damper (RIDTMD) for a spar-buoy FOWT. A device was mounted in the nacelle and designed to offer an alternative to a classic TMD. It was concluded that RIDTMD provides much better suppression of the tower side-to-side deflection, compared to a TMD, and greatly improved overall system stability.

This contribution introduces an inerter-based network that is an enhancement to the already existing TMD in the nacelle of a floating offshore wind turbine with a spar-buoy platform. The main objective is to analyse the behaviour of the FOWT model when the particular case of self-induced oscillations occurs and compare the responses of the system with classic TMD-only and the proposed inerter-based network. Through analysis, it is shown that the TMD-only model suffers the effects of the loss of the platform damping and fails to provide vibrational damping in the case of self-induced oscillations. The system with the inerter-based network, however, reduces the oscillation amplitude of the tower top and platform pitch and hence provides better vibrational control against this phenomenon.

II. SELF-INDUCED OSCILLATIONS

The self-induced oscillations are a naturally occurring phenomenon that results in the introduction of self-induced instabilities in the system, i.e., oscillations with exponentially growing oscillation amplitude. In land-based wind turbines, sufficient damping is guaranteed thanks to the fixed foundation. In contrast, as floating offshore wind turbines no longer have a fixed type of foundation, a conventional pitch-to-feather control used in the onshore structure cannot compensate for the effects of self-induced oscillations. A conventional pitch-to-feather control, referred to as blade pitch control, is a control strategy implemented in Region III of power production. In modern wind turbines, there are three operating regions (OPs) in the power production cycle:

- Region I ($0m/s$ to V_{cut-in}) where the system is in the parked condition.
- Region II (V_{cut-in} to V_{rated}), referred to as the below-rated wind region, where the control objective is to maximize power production and it is done by generator torque control.
- Region III (V_{rated} to $V_{cut-off}$), referred to as the above-rated wind region, where the control objective changes to optimal power production and the blade pitch control is implemented.

In the 5MW NREL reference wind turbine, the power generation starts at a cut-in wind speed of approximately 3-4m/s and the rated wind speed occurs at 11.4m/s. The power production is shut done at a cut-off wind velocity of 25m/s.

In the FOWTs, the self-induced oscillations can appear as a result of the change of the control objective and incorporation of the blade pitch control (between Region II and Region III). It is due to the reduction of the steady-state rotor thrust with increasing wind speed above rated values [17] and as a consequence, there is a possible decrease in the overall damping of the platform and a system may lose its damping. Based on the work by [17], the problem of self-induced oscillation in the FOWT with spar-buoy can be analysed as a rigid-body platform-pitch single-degree-of-freedom system, as shown in (2).

$$(I_{mass} + A_{radiation})\ddot{\zeta} + (B_{radiation} + B_{viscous})\dot{\zeta} + (C_{hydrostatic} + C_{lines})\zeta = L_{HH}T \quad (1)$$

The parameters in (2) are as follows: platform pitch angle ζ in $rads$, platform pitch rotational velocity $\dot{\zeta}$ in $rads/s$, platform pitch rotational acceleration $\ddot{\zeta}$ in $rads/s^2$, pitch inertia associated with wind turbine and barge mass I_{mass}, added inertia (added mass) associated with hydrodynamic radiation in pitch $A_{radiation}$, damping associated with hydrodynamic radiation in pitch $B_{radiation}$, linearized damping associated with hydrodynamic viscous drag in pitch $B_{viscous}$, hydrostatic restoring in pitch $C_{hydrostatic}$, linearized hydrostatic restoring in pitch from all mooring lines C_{lines}, hub height L_{HH} and aerodynamic rotor thrust T.

Equation (2) is a general expression governing the self-induced oscillation problem. The same equation, however, can be expressed in terms of the transnational displacement of the hub ($x = L_{HH} \times \zeta$) and the thrust sensitivity ($\frac{\partial T}{\partial V}$) to visualise better the relationship the trust reduction has on the loss of platform damping. Equation (2) shows the results of

Fig. 1. 5MW NREL with OC3-Hywind spar buoy platform [20].

the substitution where T_0 is the aerodynamic rotor thrust at the linearization point and V is rotor-disk-averaged wind speed.

$$\underbrace{\left(\frac{I_{mass}+A_{radiation}}{L_{HH}^2}\right)}_{M_x}\ddot{x}+\underbrace{\left(\frac{B_{radiation}+B_{viscous}}{L_{HH}^2}+\frac{\partial T}{\partial V}\right)}_{C_x}\dot{x} + \underbrace{\left(\frac{C_{hydrostatic}+C_{lines}}{L_{HH}^2}\right)}_{K_x}x=T_0 \tag{2}$$

It is now evident that the overall damping coefficient C_x contains the thrust sensitivity term $\frac{\partial T}{\partial V}$. Therefore, if the rotor thrust decreases for increasing wind speeds in the above-rated wind region, the system may see its damping properties reduced if

$$|\frac{B_{radiation}+B_{viscous}}{L_{HH}^2}|<|\frac{\partial T}{\partial V}|.$$

As discussed previously, self-induced oscillations pose a unique challenge in floating offshore wind turbines as structural instabilities may be introduced. Hence, it is desired to study this phenomenon in order to propose control strategies capable of counteracting it [17]–[19].

III. MODEL DESCRIPTION

In this work, a 5MW NREL wind turbine with an OC3-Hywind spar buoy platform is used (Fig. 1) [20]. The 5MW baseline wind model is a conventional three-bladed upwind variable-speed blade-pitch-to-feather-controlled turbine [21]. This benchmark was used by many international researchers [17], [22]–[28].

It is crucial to highlight that the dynamic model of the FOWT requires the following assumptions [29]:

- The system's structure is agreed to be represented as a 3DOFs system consisting of a spar-buoy platform, tower and rotor nacelle assembly with TMD. Any dynamics or motion coming from the rotor yaw, generator or gearbox are neglected.
- The tower flexibility is represented by a linear rigid rotating beam hinged at the tower bottom [30].
- The model is fully isolated from any external environmental factors e.g., wind, waves or currents.

A. Baseline Model with TMD

Based on Lagrange's approach for a non-conservative system with n generalized coordinates, a dynamic equation of motion for the FOWT with a spar-buoy foundation can be derived.

$$\frac{d}{dt}\left(\frac{\partial L}{\partial \dot{q}_i}\right)-\left(\frac{\partial L}{\partial q_i}\right)=Q_i \quad (i=1,2,\ldots,n) \tag{3}$$

$$L=T-V \tag{4}$$

The parameters in (3) and (4) are the generalized non-potential force Q_i, total kinetic energy of the system T, total potential energy of the system V and Lagrange operator L.

By application of Lagrange's method and by the assumption of the small angle approximation, the full model of the FOWT with a spar-buoy platform can be derived as follows:

$$\begin{cases} I_p\ddot{\theta}_p=-d_p\dot{\theta}_p-k_p\theta_p-m_pgR_p\theta_p+k_t(\theta_t-\theta_p)+ \\ d_t(\dot{\theta}_t-\dot{\theta}_p) \\ \\ I_t\ddot{\theta}_t=m_tgR_t\theta_t-k_t(\theta_t-\theta_p)-d_t(\dot{\theta}_t-\dot{\theta}_p) \\ -m_Tg(R_T\theta_t-x_T)-k_TR_T(R_T\theta_t-x_T)- \\ d_TR_T(R_T\dot{\theta}_t-\dot{x}_T) \\ \\ m_T\ddot{x}_T=k_T(R_T\theta_t-x_T)+d_T(R_T\dot{\theta}_t-\dot{x}_T)+m_Tg\theta_t \end{cases} \tag{5}$$

In (5), the model parameters are as follows: gravitational acceleration g, platform inertia I_p, mass of the platform rigid body m_p, platform centre of mass R_p, platform flexibility k_p, platform torsion properties d_p, tower inertia I_t, mass of the tower rigid body m_t, tower centre of mass R_t, tower flexibility k_t, tower torsion properties d_t, mass of the TMD inside nacelle m_T, TMD centre of mass R_T, TMD spring coefficient k_T and TMD damping coefficient d_t.

Some model parameters can be taken from the OpenFAST input file i.e., g= 9.81m/s^2, R_p= 89.9155m, R_t= 60.5961m, m_p= 7466330kg and m_t= 599718kg. The remaining parameters i.e., I_p, k_p, d_p, I_t, k_t and d_t are identified by application of the Nelder-Mead simplex algorithm as described in [31] with the objective function being a sum of squares between the author's model tower top displacement (TTD) and tower top displacement TTDspFA from the OpenFAST output file:

$$objective=\sum(TTD-TTDspFA)^2.$$

Table I and Fig. 2 show the results of the benchmark model parameter identification.

TABLE I
BENCHMARK MODEL PARAMETER IDENTIFICATION

Parameters:	Values:
I_p $[kg \cdot m^2]$	5.57×10^{10}
k_p $[kg \cdot m^2/s^2]$	-5.56×10^9
d_p $[kg \cdot m^2/s]$	3.93×10^8
I_t $[kg \cdot m^2]$	3.5×10^9
k_t $[kg \cdot m^2/s^2]$	1.88×10^{10}
d_t $[kg \cdot m^2/s]$	5.82×10^7

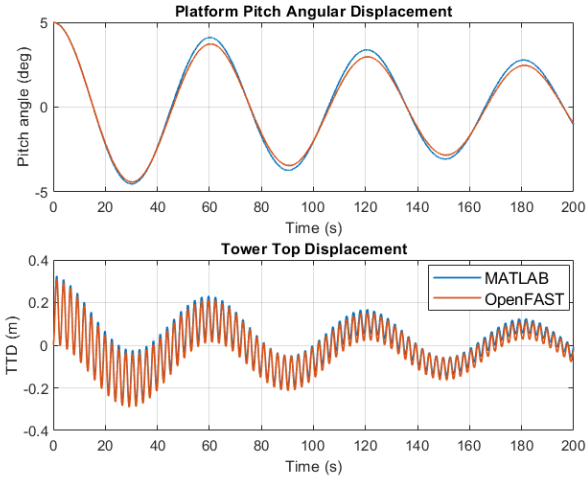

Fig. 2. Validation of authors' model with OpenFAST 5MW NREL benchmark model with spar-buoy foundation.

The next step was to repeat the system parameter identification when the TMD is considered together with the benchmark model. The algorithm and objective function remained unchanged as in the benchmark parameter identification case. The known parameters are the fixed TMD mass m_T= 40000kg and the centre of the TMD mass R_T= 80.6m. Furthermore, the TMD parameters obtained through parameter estimation are optimized to further improve the model's response. The optimized TMD parameters are obtained by application of the surrogate optimization algorithm as described in [32] with the objective function to minimize the tower top displacement. The resultant plots are shown in Fig. 3. Table II shows the cumulative results for both the parameter estimation and parameter optimization of the TMD in the nacelle.

The misalignments in the obtained responses are the result of the assumption made i.e., the tower is represented as a rigid body whereas in OpenFAST the tower is a flexible body. However, these misalignments do not interfere with the stability analysis done in this work.

TABLE II
TMD MODEL PARAMETERS

Parameter estimation:	Values:
k_T $[kg \cdot m^2/s^2]$	41618.72
d_T $[kg \cdot m^2/s]$	29504.36
Parameter optimization:	**Values:**
k_T $[kg \cdot m^2/s^2]$	1000.00
d_T $[kg \cdot m^2/s]$	15816.32

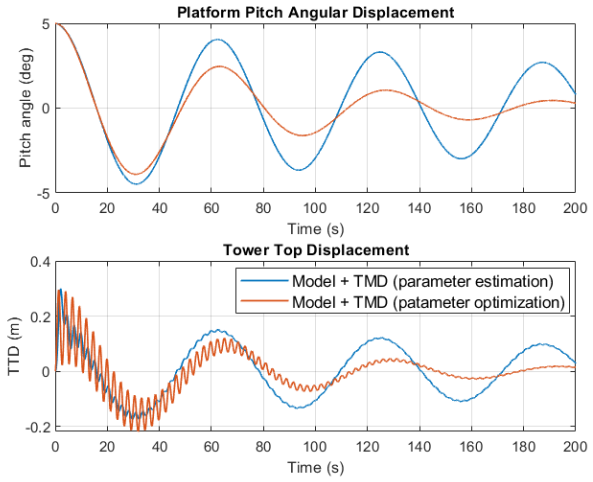

Fig. 3. Comparison of model with TMD parameters from parameter estimation and parameter optimization.

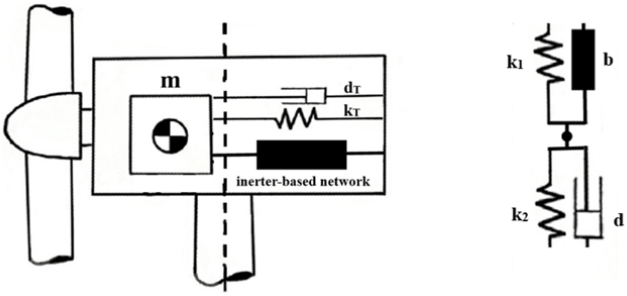

Fig. 4. Inerter-based network in the nacelle

B. Structure with Inerter-Based Network

This contribution proposes an inerter-based network as an additional control device complimenting the classic TMD which is installed in the nacelle of the 5MW FOWT with a spar-buoy foundation, as illustrated in Fig. 4. The main objective of network installation is to counter the self-induced disturbances appearing on the structure as a consequence of the loss of the damping in the spar, as explained in Section II.

As introduced by [10], the inerter produces a force that is proportional to the relative acceleration between its terminals as shown in (6) where b is the inertance and $\ddot{x}_2$, $\ddot{x}_1$ are two corresponding displacements.

$$F_{inerter} = b(\ddot{x}_2 - \ddot{x}_1) \tag{6}$$

As shown in Fig. 4, the proposed inerter-based network consists of the inerter with inertance b, damper with damping coefficient d and two springs with stiffnesses k_1 and k_2. The mass of the newly introduced network m remains unchanged

TABLE III
INERTER-BASED NETWORK MODEL PARAMETER OPTIMIZATION

Parameters:	Values:
b $[kg]$	99999680
d $[kg \cdot m^2/s]$	1000
k_1 $[kg \cdot m^2/s^2]$	999997.75
k_2 $[kg \cdot m^2/s^2]$	10000
d_T $[kg \cdot m^2/s]$	10000
k_T $[kg \cdot m^2/s^2]$	850

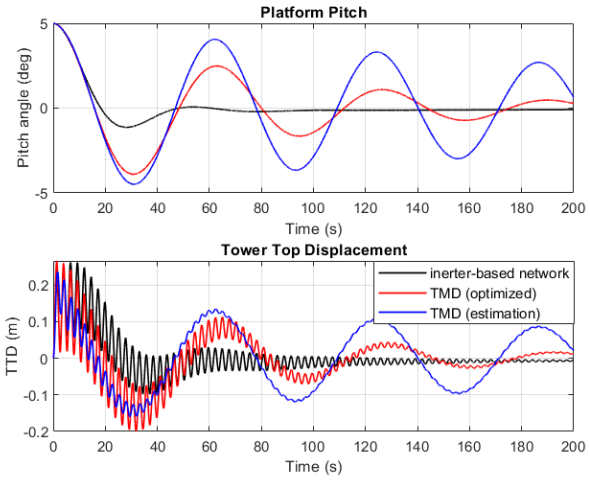

Fig. 5. Comparison plots of the model with inerter-based network, model with optimized TMD and model with original TMD (from estimation).

and equal to m_T, hence the centre of the network mass also remains as R_T.

The equation of motion for the structure with the inerter-based network can be obtained by adequate modification of (5) by consideration of new elements and by taking into account the 4th DOF as shown in (7).

$$F_{inerter} + F_{spring,1} = F_{damper} + F_{spring,2} \tag{7}$$

The generalized pattern search (GPS) algorithm is used to identify the inerter-based network parameters i.e., b, d, k_1 and k_2. The TMD parameters k_T and d_T, obtained from the surrogate optimization (refer to Table II), are also considered in the GPS optimization loop. The initial guesses for the algorithm are taken from the interior-point method (IPM) as described in [33]. The objective function again is to minimise the tower top displacement. Table III summarises the results of the parameter optimization and Fig. 5 shows the model's response.

IV. ANALYSIS OF MODEL RESPONSE UNDER SELF-INDUCED OSCILLATIONS

As it is evident from Fig. 5, the proposed inerter-based network provides the greatest oscillation amplitude reduction compared to the model with classic TMD-only. This beneficial impact can be seen for platform pitch and tower top displacement. Following these results, the inerter-based network is analysed to study its behaviour under self-induced oscillations. The phenomenon was recreated in MATLAB by consideration of the explanation provided in Section II and the estimation of the damping ratios during the wind turbine power production cycle derived by [17].

TABLE IV
SUPPRESSION RATE BETWEEN INERTER-BASED NETWORK AND CLASSIC TMD

Wind velocity:	12m/s	13m/s	14m/s	15m/s
Suppression rate [%]:	90.56	75.74	57.57	45.34

A. Time Domain Analysis

As mentioned previously, the proposed network has been tested within the range of wind velocities of interest where the occurrence of self-induced oscillation is possible i.e., from V_{rated}, when the change of the control objective takes place, up to approximately 15m/s. The model is simulated with the initial platform pitch of $5°$. Fig. 6 and Fig. 7 show the comparison of the responses of the system with the inerter-based network and with TMD-only in the wind velocity range of 12-14m/s over 500s time interval when the effects of self-induced disturbances are the most prominent. Fig. 8 is a close-up of the response of the model with TMD-only in the time interval of 150s, this helps to better visualise the growing oscillation amplitude when the wind turbine platform experiences loss of damping.

It is evident that due to the implementation of the inerter-based network into a classic TMD, the effects of self-induced oscillations are damped and the oscillation amplitude is significantly reduced for both platform pitch and tower top. To quantify these improvements, the suppression rate is calculated as shown in (8) where SD stands for standard deviation. Table IV is a summary of the obtained suppression rates at wind velocity range of interest 12-15m/s.

$$\frac{SD(TTD_{TMD}) - SD(TTD_{\text{inerter-based network}})}{SD(TTD_{TMD})} \times 100\% \tag{8}$$

Table IV shows a performance improvement of over 90% at 12m/s, when the inerter-based network is compared to the model with TMD-only, and up to 45% at wind velocity 15m/s.

An alternative way to observe the improvements the inerter-based network introduces to the model concerning its stability is by plotting eigenvalues evolutions. To do so, two root loci for a full power production cycle (wind velocity range from 4m/s to 24m/s) are drawn for both models. The resultant plots are shown in Fig. 9a, where the TMD-only model is indicated in blue and the inerter-based model is in black. The initial eigenvalues for wind speed of 4m/s are marked by the red square whereas the final eigenvalues at 24m/s are pink diamonds. It is evident that the eigenvalues of the inter-based network model do not cross zero to the right-hand side (RHS) of the plot and remain on the left part of the imaginary

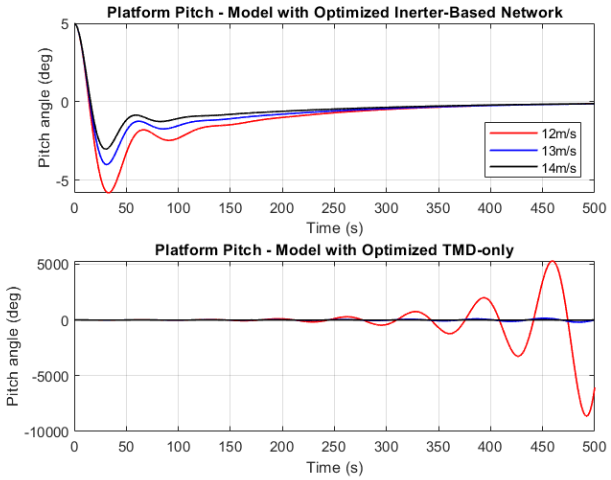

Fig. 6. Platform pitch comparison response of the model with the inerter-based network vs model with TMD-only under self-induced oscillations.

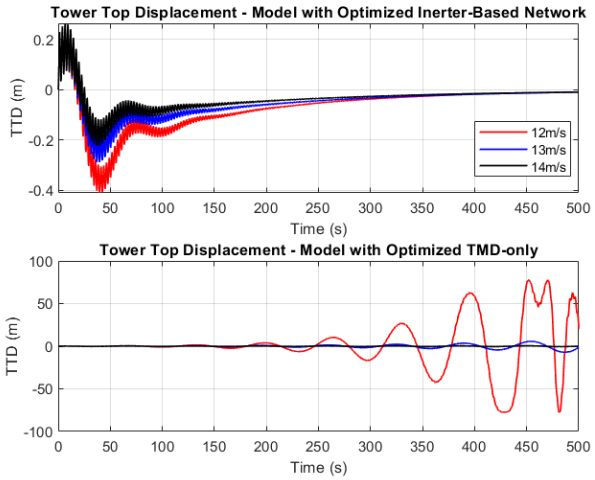

Fig. 7. Tower top displacement comparison response of the model with the inerter-based network vs model with TMD-only under self-induced oscillations.

plane (LHS), indicating stability. In comparison, the model with TMD-only becomes unstable and crosses to the RHS at the rated wind speed. Hence, it can be concluded that implementation of the inerter-based network assures that the system remains stable (on the LHS plane of the root locus) despite the occurrence of self-induced oscillations. Fig. 9b shows the close-up of the path of one of the eigenvalues to demonstrate evidence of changes in the imaginary component of evolution.

V. CONCLUSIONS

In this contribution, the authors present a passive inerter-based network in the 5MW NREL FOWT with a spar-buoy foundation. This network is the enhancement of the already existing in the nacelle classic TMD. The main objective of this work was to stabilize the system experiencing self-induced oscillations as a result of possible loss of platform damping

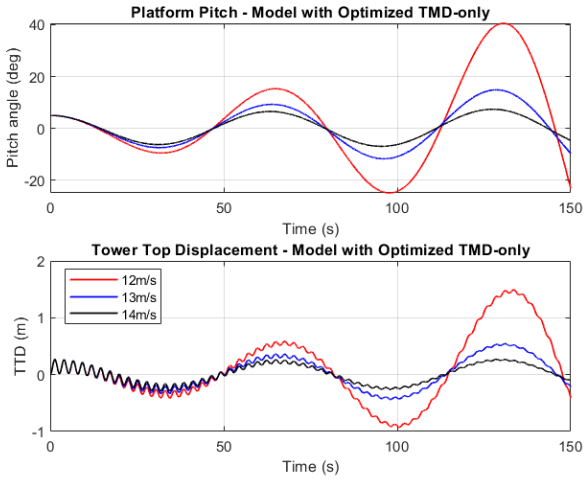

Fig. 8. Close-up of the TMD-only model response under self-induced oscillations.

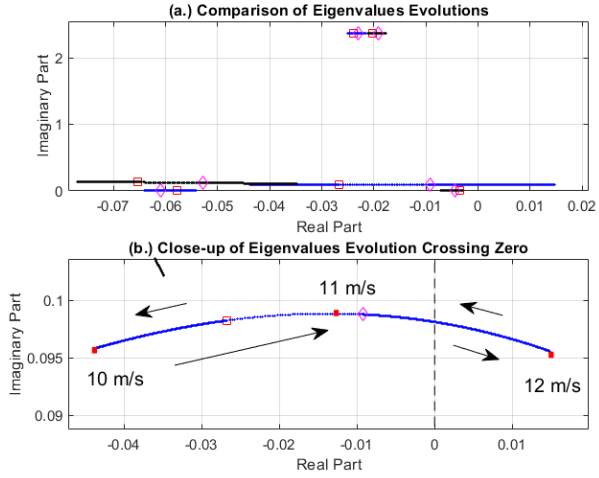

Fig. 9. (a.) Eigenvalues evolutions of classic TMD (blue line) and model enhanced by the inerter-based network (black line); (b.) Close-up of the eigenvalue of interest that crosses the stability axis at V_{rated} when the system is fitted with classic TMD only.

and reduce its oscillation amplitude. A 4DOFs dynamic model of FOWT with the ineretr-based network was derived and optimized. The key highlights of this work can be summarised as follows:

- In a free decay test, the amplitude of oscillation of both the tower top and platform pitch is reduced due to the introduction of the inerter-based network.
- In the case of self-induced oscillations, there is a reduction of the self-induced oscillation amplitude of both the tower top and platform pitch, with up to 90.56% supression at a wind velocity of 12m/s for the tower top.
- The root loci analysis shows that the inerter-based network never crosses zero to the RHS of the plane which guarantees system stability in the particular case of self-induced oscillations.

In conclusion, the implementation of an inerter in the spar-buoy FOWT can positively influence the dynamic behaviour of the structure by means of the reduction of the unwanted oscillations appearing at the structure, in the case of the occurrence of self-induced oscillations. The proposed inerter-based network guarantees stability and significantly reduces oscillation amplitude. As a future work, there could be numerous different combinations of inerter-based networks tested with possibility of implementation of semi-active control.

ACKNOWLEDGMENT

S.P. thanks Dr Agathoklis Giaralis for his useful advice and insight on the inerter use and implementation.

REFERENCES

[1] IEA, "Global energy review 2021," 2021.
[2] G. W. E. Council, "Floating offshore wind- a global opportunity," 2022.
[3] B. Spencer and M. K. Sain, "Controlling buildings: a new frontier in feedback," *IEEE Control Systems Magazine*, vol. 17, no. 6, pp. 19–35, 1997.
[4] H. Adeli and A. Saleh, "Integrated structural/control optimization of large adaptive/smart structures," *International Journal of Solids and Structures*, vol. 35, no. 28-29, pp. 3815–3830, 1998.
[5] H. Adeli, "Smart structures and building automation in the 21st century," in *International symposium on automation in construction*, vol. 25, 2008, pp. 5–10.
[6] C.-L. Lee, Y.-T. Chen, L.-L. Chung, and Y.-P. Wang, "Optimal design theories and applications of tuned mass dampers," *Engineering structures*, vol. 28, no. 1, pp. 43–53, 2006.
[7] C.-C. Lin and J.-F. Wang, "Optimal design and practical considerations of tuned mass dampers for structural control," in *Design Optimization of Active and Passive Structural Control Systems*. IGI global, 2013, pp. 126–149.
[8] Y. Si, H. R. Karimi, and H. Gao, "Modeling and parameter analysis of the oc3-hywind floating wind turbine with a tuned mass damper in nacelle," *Journal of Applied Mathematics*, vol. 2013, 2013.
[9] M. Ha and C. Cheong, "Pitch motion mitigation of spar-type floating substructure for offshore wind turbine using multilayer tuned liquid damper," *Ocean Engineering*, vol. 116, pp. 157–164, 2016.
[10] M. C. Smith, "Synthesis of mechanical networks: the inerter," *IEEE Transactions on automatic control*, vol. 47, no. 10, pp. 1648–1662, 2002.
[11] M. C. Smith, "The inerter: a retrospective," *Annual Review of Control, Robotics, and Autonomous Systems*, vol. 3, pp. 361–391, 2020.
[12] R. Zhang, M. Wu, C. Pan, C. Wang, and L. Hao, "Design of mdof structure with damping enhanced inerter systems," *Bulletin of Earthquake Engineering*, vol. 21, no. 3, pp. 1685–1711, 2023.
[13] S. Sarkar and B. Fitzgerald, "Vibration control of spar-type floating offshore wind turbine towers using a tuned mass-damper-inerter," *Structural Control and Health Monitoring*, vol. 27, no. 1, p. e2471, 2020.
[14] B. Fitzgerald, J. McAuliffe, S. Baisthakur, and S. Sarkar, "Enhancing the reliability of floating offshore wind turbine towers subjected to misaligned wind-wave loading using tuned mass damper inerters (tmdis)," *Renewable Energy*, vol. 211, pp. 522–538, 2023.
[15] S. Sarkar and B. Fitzgerald, "Fluid inerter for optimal vibration control of floating offshore wind turbine towers," *Engineering Structures*, vol. 266, p. 114558, 2022.
[16] Z. Zhang and C. Høeg, "Inerter-enhanced tuned mass damper for vibration damping of floating offshore wind turbines," *Ocean Engineering*, vol. 223, p. 108663, 2021.
[17] J. Jonkman, "Influence of control on the pitch damping of a floating wind turbine," in *46th AIAA aerospace sciences meeting and exhibit*, 2009, p. 1306.
[18] T. J. Larsen and T. D. Hanson, "A method to avoid negative damped low frequent tower vibrations for a floating, pitch controlled wind turbine," in *Journal of Physics: Conference Series*, vol. 75, no. 1. IOP Publishing, 2007, p. 012073.
[19] S. Piernikowska, M. Tomas-Rodriguez, and M. S. Peñas, "Floating offshore wind turbine stability study under self-induced vibrations," *Trends in Maritime Technology and Engineering*, pp. 445–450, 2022.
[20] J. Jonkman, "Definition of the floating system for phase iv of oc3," National Renewable Energy Lab.(NREL), Golden, CO (United States), Tech. Rep., 2010.
[21] J. Jonkman, S. Butterfield, W. Musial, and G. Scott, "Definition of a 5-mw reference wind turbine for offshore system development," National Renewable Energy Lab.(NREL), Golden, CO (United States), Tech. Rep., 2009.
[22] J. M. Jonkman, *Dynamics modeling and loads analysis of an offshore floating wind turbine*. University of Colorado at Boulder, 2007.
[23] V.-N. Dinh and B. Basu, "Passive control of floating offshore wind turbine nacelle and spar vibrations by multiple tuned mass dampers," *Structural Control and Health Monitoring*, vol. 22, no. 1, pp. 152–176, 2015.
[24] M. Santos and M. Tomás-Rodríguez, "Floating offshore wind turbines: Controlling the impact of vibrations," in *7th International Conference on Systems and Control, Valencia Spain*, 2018.
[25] M. A. Lackner and M. A. Rotea, "Passive structural control of offshore wind turbines," *Wind energy*, vol. 14, no. 3, pp. 373–388, 2011.
[26] M. A. Lackner and M. A. Rotea, "Structural control of floating wind turbines," *Mechatronics*, vol. 21, no. 4, pp. 704–719, 2011.
[27] G. M. Stewart and M. A. Lackner, "The effect of actuator dynamics on active structural control of offshore wind turbines," *Engineering Structures*, vol. 33, no. 5, pp. 1807–1816, 2011.
[28] H. Namik, M. Rotea, and M. Lackner, "Active structural control with actuator dynamics on a floating wind turbine," in *51st AIAA Aerospace Sciences Meeting Including the New Horizons Forum and Aerospace Exposition*, 2013, p. 455.
[29] G. M. Stewart, "Load reduction of floating wind turbines using tuned mass dampers," 2012.
[30] G. Stewart and M. Lackner, "Determining optimal tuned mass damper parameters for offshore wind turbines using a genetic algorithm," in *50th AIAA aerospace sciences meeting including the new horizons forum and aerospace exposition*, 2012, p. 376.
[31] J. C. Lagarias, J. A. Reeds, M. H. Wright, and P. E. Wright, "Convergence properties of the nelder–mead simplex method in low dimensions," *SIAM Journal on optimization*, vol. 9, no. 1, pp. 112–147, 1998.
[32] MATLAB, "surrogateopt," 2023. [Online]. Available: https://uk.mathworks.com/help/gads/surrogateopt.html
[33] MATLAB, "fmincon," 2023. [Online]. Available: https://uk.mathworks.com/help/optim/ug/fmincon.html